VERTEX RECONSTRUCTION AND TRACKING WITH THE $\bar{\text{P}}$ANDA MICRO-VERTEX-DETECTOR

Simone Bianco

L PANDA COLLABORATION MEETING

10.09.2014

universitätbonn

Bonn-Cologne Graduate School of Physics and Astronomy

Outline

- The Micro-Vertex-Detector
- Implementation of the MVD geometry
- Vertex reconstruction characterization
- Tracking station with prototype sensors
- Benchmark physics channel $\Lambda^{+}_{C} \rightarrow pK^{-}\pi^{+}$

The Micro-Vertex-Detector

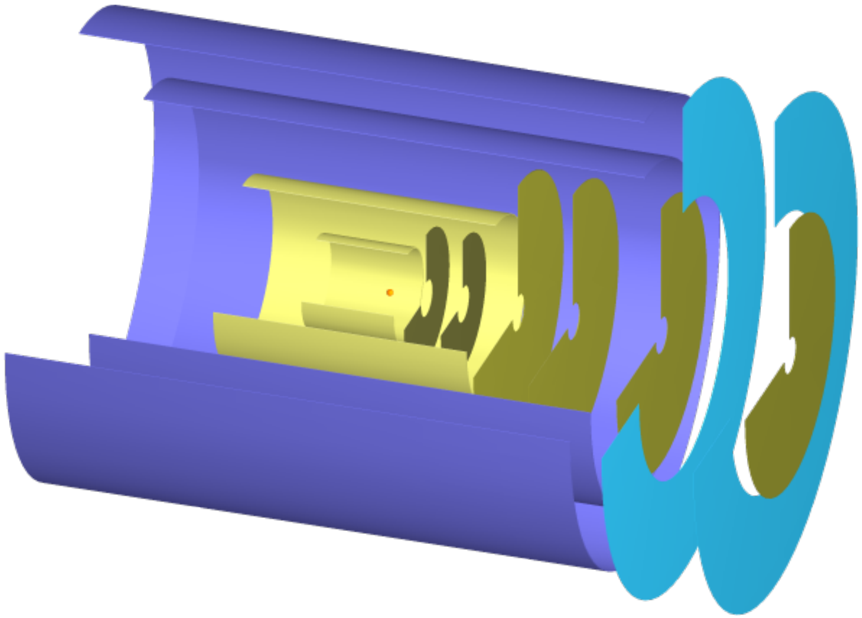

Requirements:

- Vertex resolution (< 100 µm)
- Momentum reconstruction
- High rates capability (~10 kHz/ch)
- High radiation tolerance (10 Mrad, 10^{13}-10^{14} $n_{1\ MeV\ eq}/cm^2$)
- Trigger-less read-out

Two barrel equipped with pixel sensors surrounded by two strip layers.

Six forward pixel disks and two strip wheels.

The MVD Sensors - Pixels

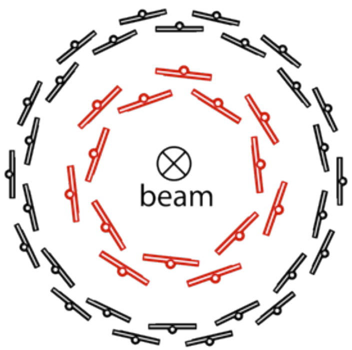

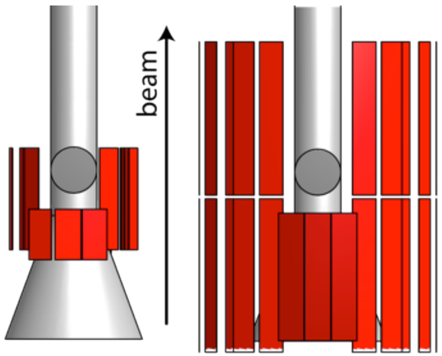

Two barrel layers composed of modular staves.

Six forward disks (2 small and 4 large).

100 µm x 100 µm pixel cells bump bonded to a custom trigger-less front-end chip (ToPiX).

Sensors realized with epitaxial silicon grown on Czochralski(Cz)-substrate.

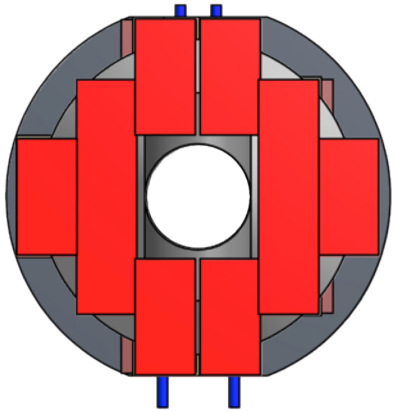

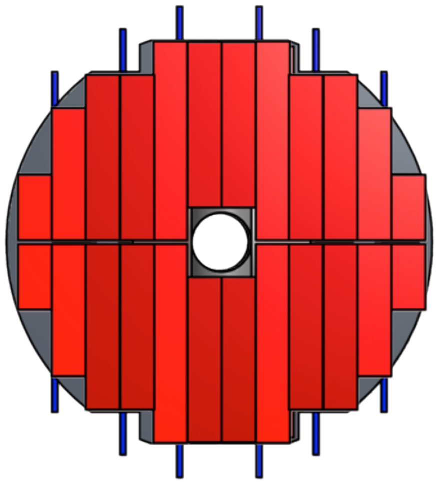

The MVD Sensors - Strips

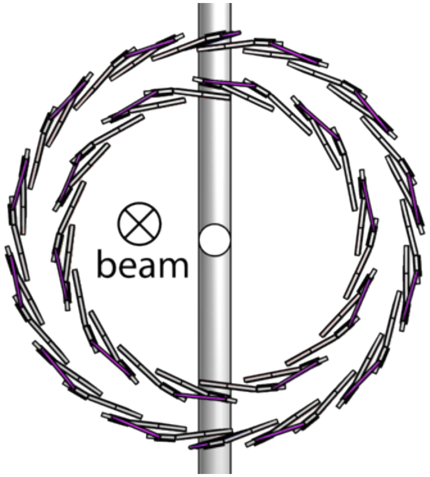

Two barrel layers and two forward wheels covering large radii.

65 (barrel) or 130 µm (wheel) strip pitch.

Custom trigger-less read-out chip.

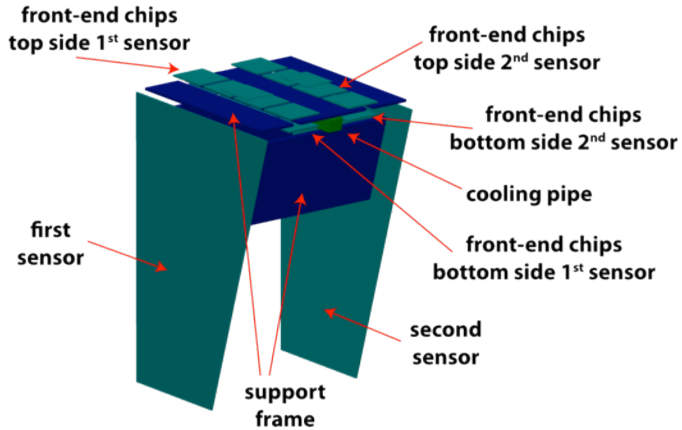

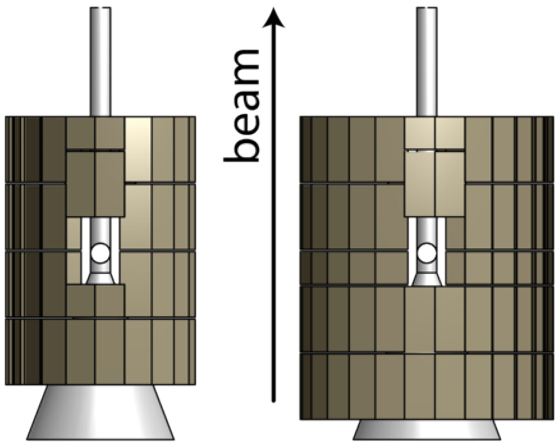

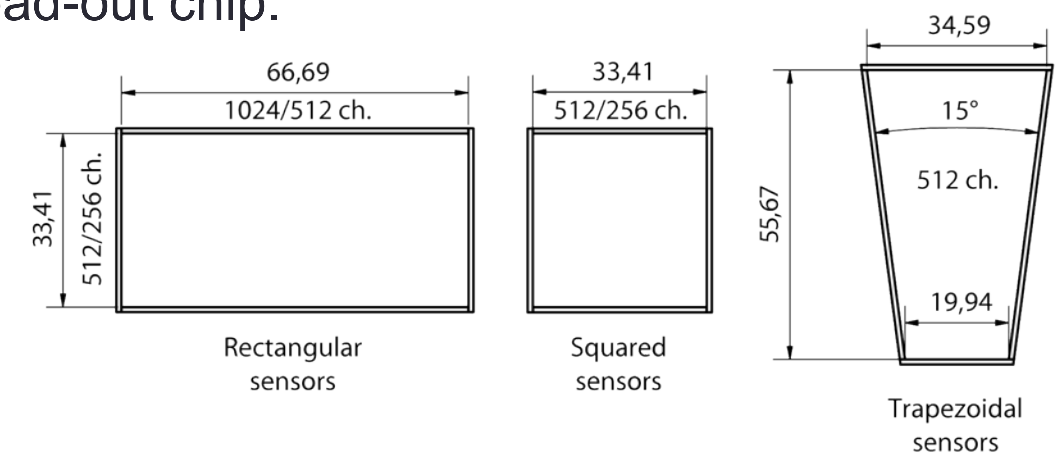

The MVD Geometry for Monte-Carlo Simulations

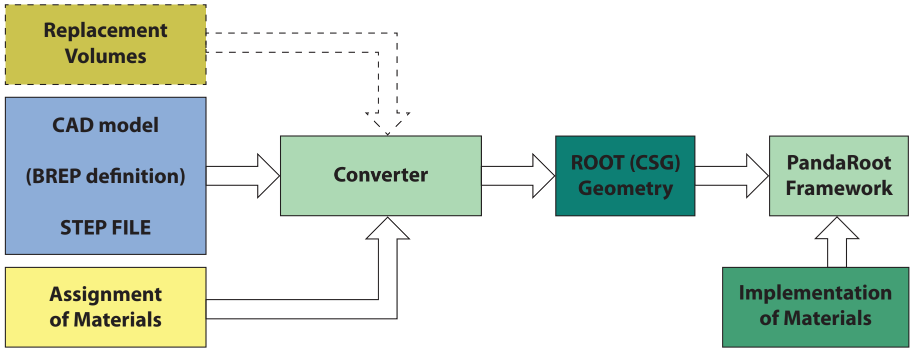

Aim: Introduce a realistic geometry of the detector within the simulation framework including both active and passive materials.

Flexible solution to link mechanical development to detector studies.

Complex shapes were implemented as a collection of simpler volumes.

Materials were tagged during the conversion and implemented in the framework.

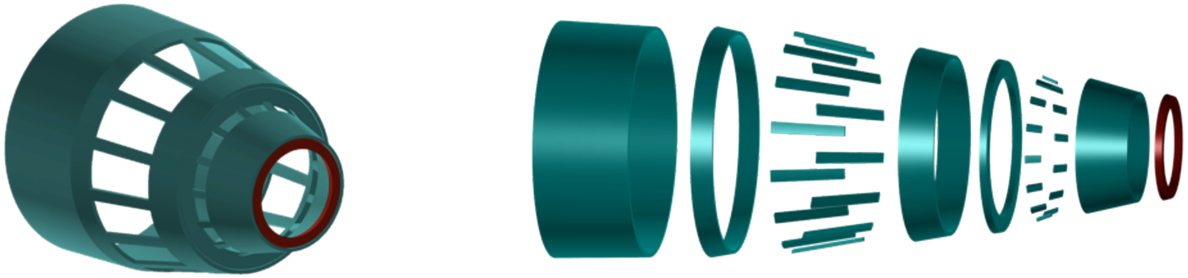

S. Bianco, T. Würschig, T. Stockmanns, K.-Th. Brinkmann, "*The CAD model of the PANDA Micro-Vertex-Detector in physics simulations*", Nucl. Instr. Meth. A, 654 (2011) 630-633, http://dx.doi.org/10.1016/j.nima.2011.05.021

MVD-2.1 Model

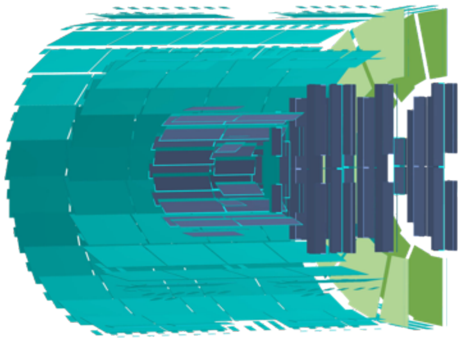

Sensors and front-end chips

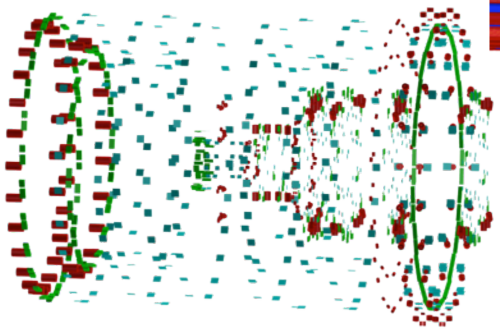

Capacitors and electronic components

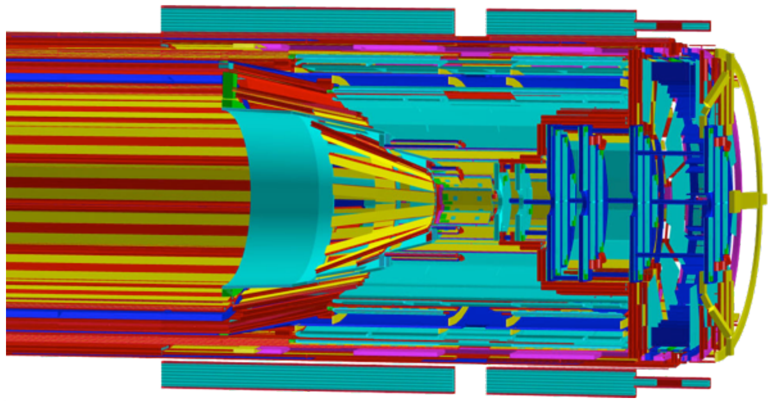

Full geometry (side view)

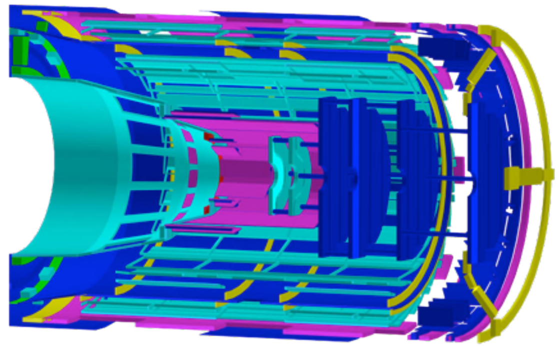

Support structures

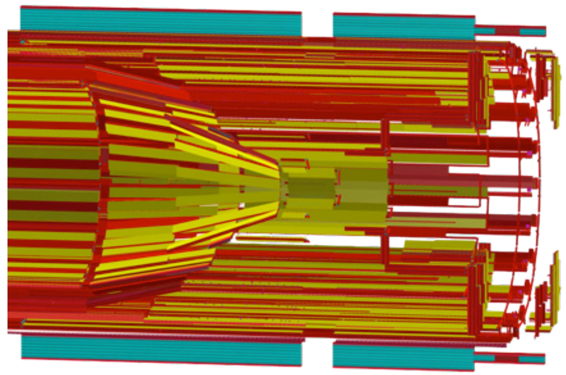

Services

Characterization of the MVD Model

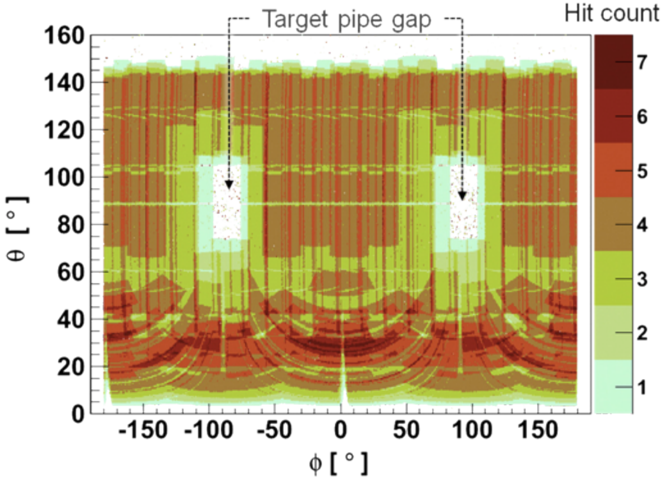

1 GeV/c π^+
from (0,0,0)
2 T field

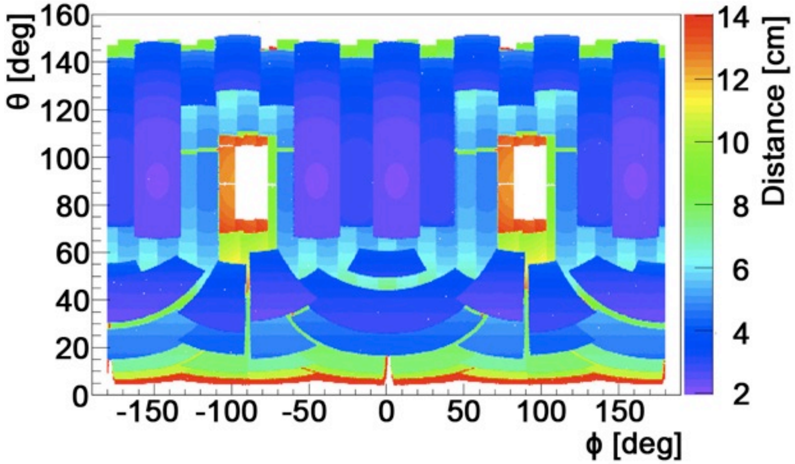

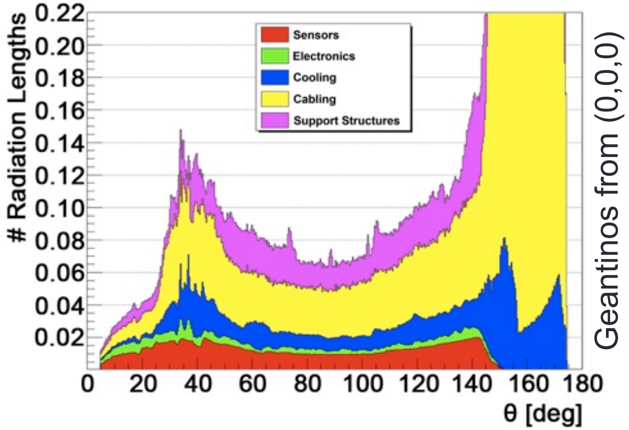

In most of the detector acceptance:

- At least 4 MVD hit points
- Max 4 cm between the interaction point (IP) and the first measured hit point
- Total material budget below 10% X_0

S. Bianco on behalf of the PANDA MVD group, “*Characterization of the PANDA Micro-Vertex-Detector and Analysis of the First Data Measured with a Tracking Station*”, IEEE NSS Record N42 (278), 2010, 1149-1152

Vertex Reconstruction Performance

A vertex resolution better than 100 μm is required to tag short-lived particle decays.

The vertex reconstruction has been tested with two kind of studies:

1. Four pions homogeneously distributed within the acceptance
2. Primary vertex in the p p → ψ (2S) →J/ψ $\pi^+\pi^-$ reaction

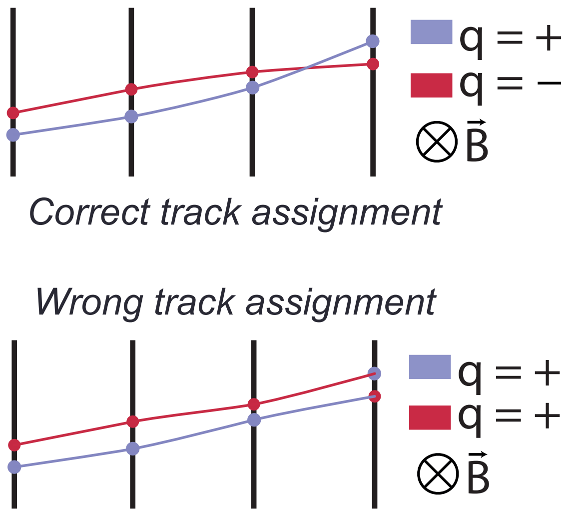

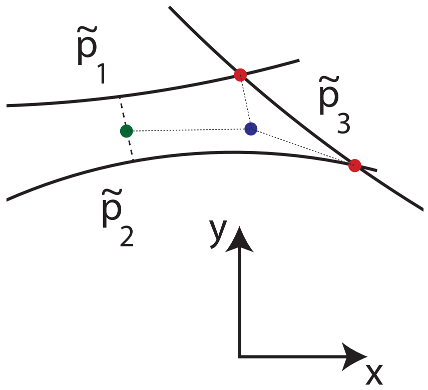

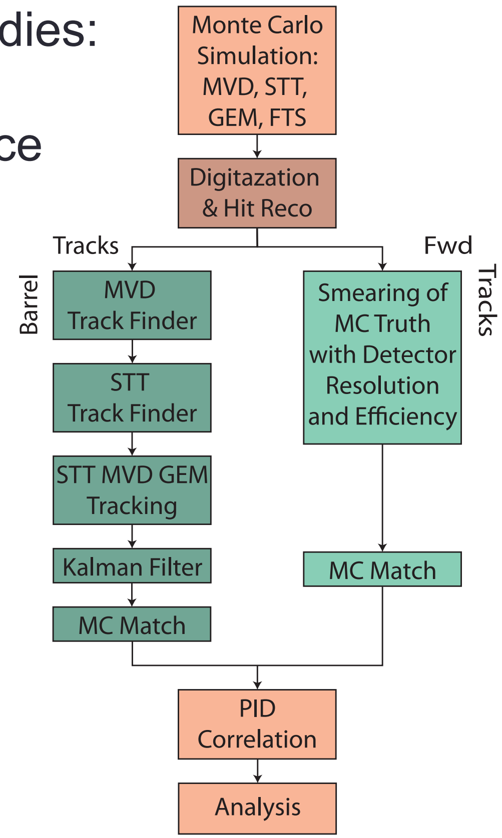

S. Bianco on behalf of the PANDA MVD group, "*Beam Tests and Performance Studies for the PANDA Micro-Vertex-Detector*", IEEE NSS Record N14(219), 2012, 1503-1508

Four Pion Scans

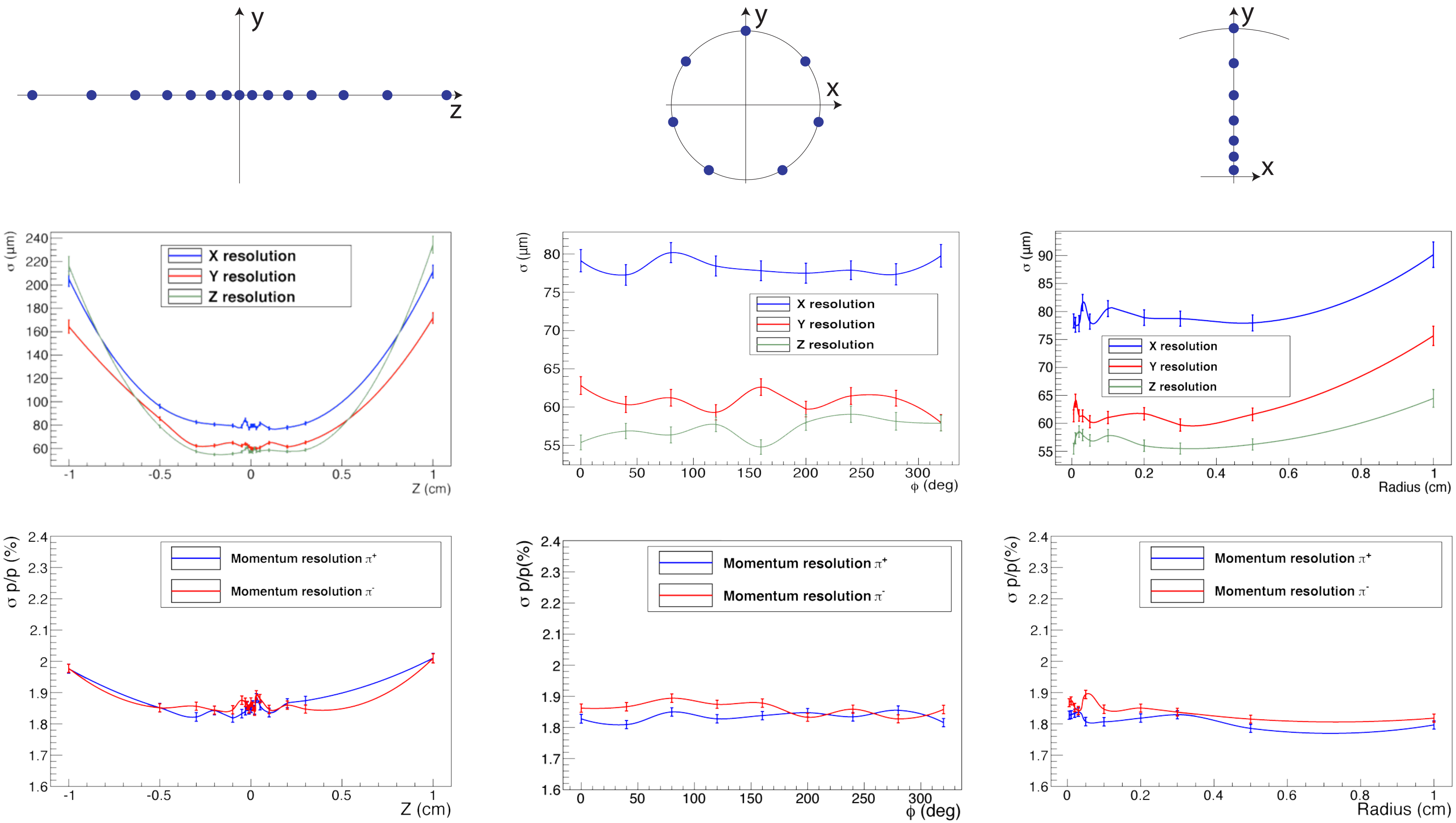

Particle Decays

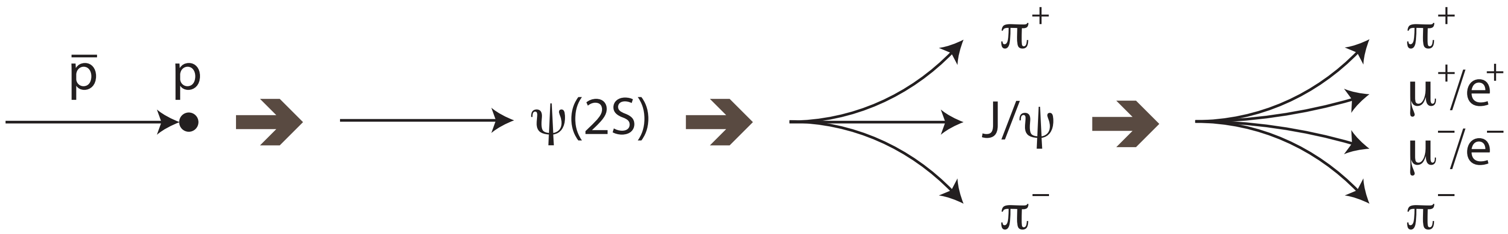

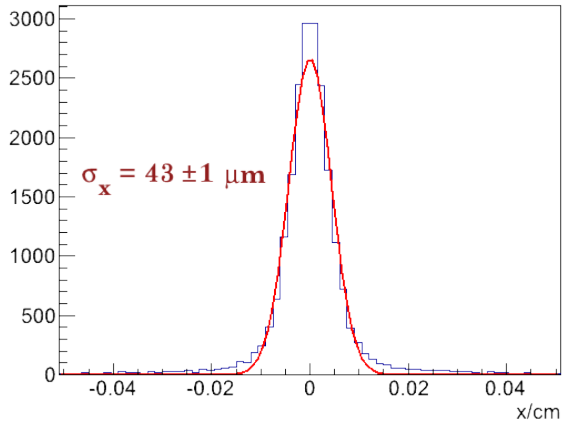

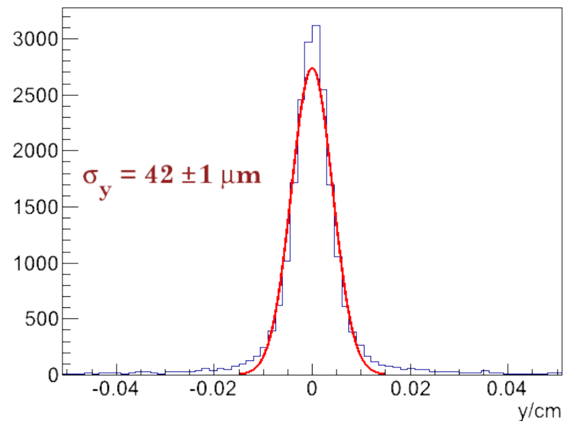

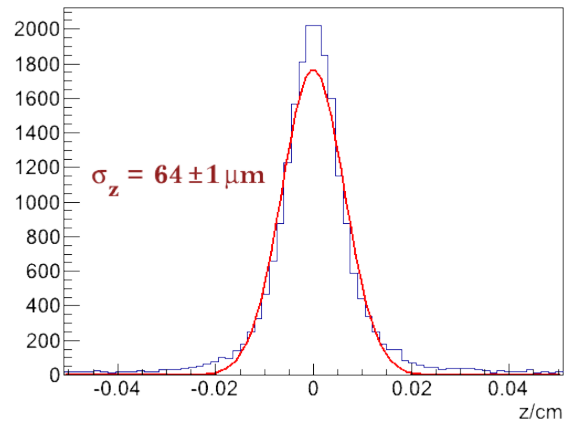

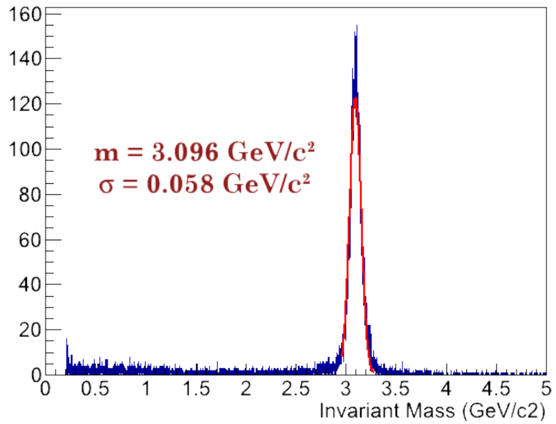

$J/\psi \rightarrow \mu^+\mu^-$ reconstructed vertices, invariant and missing mass.

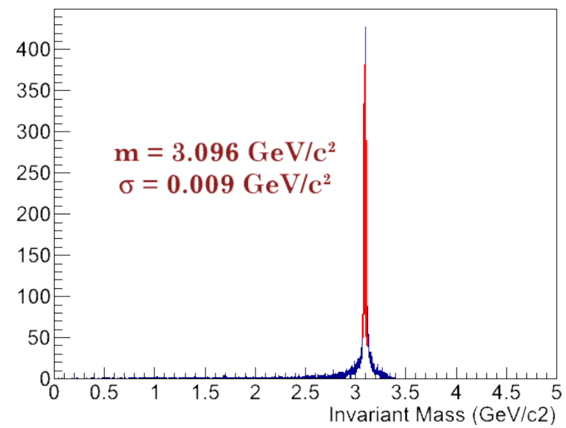

Particle Decays

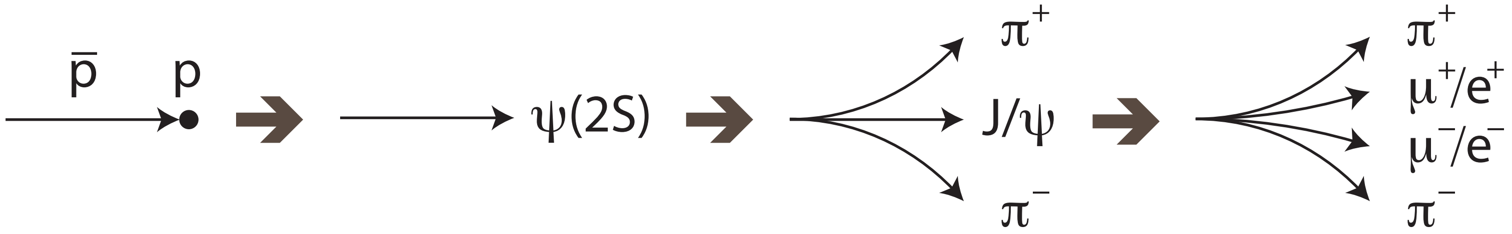

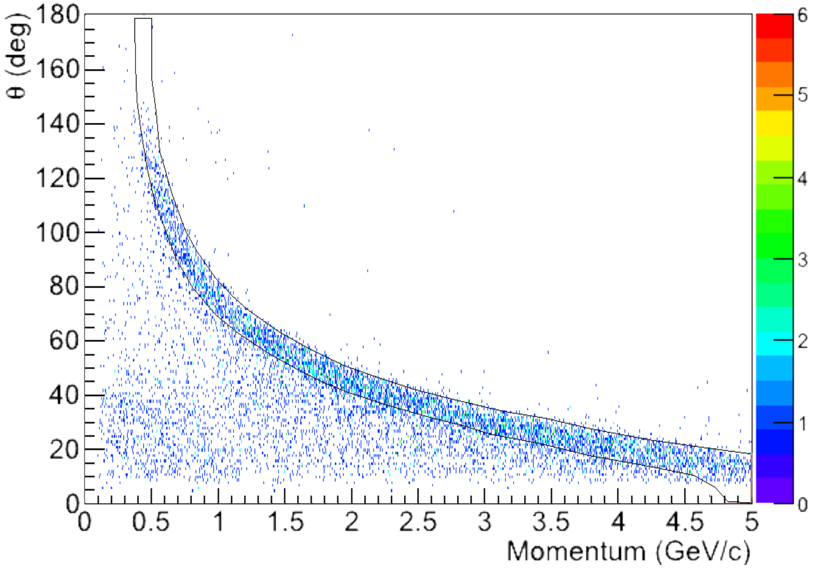

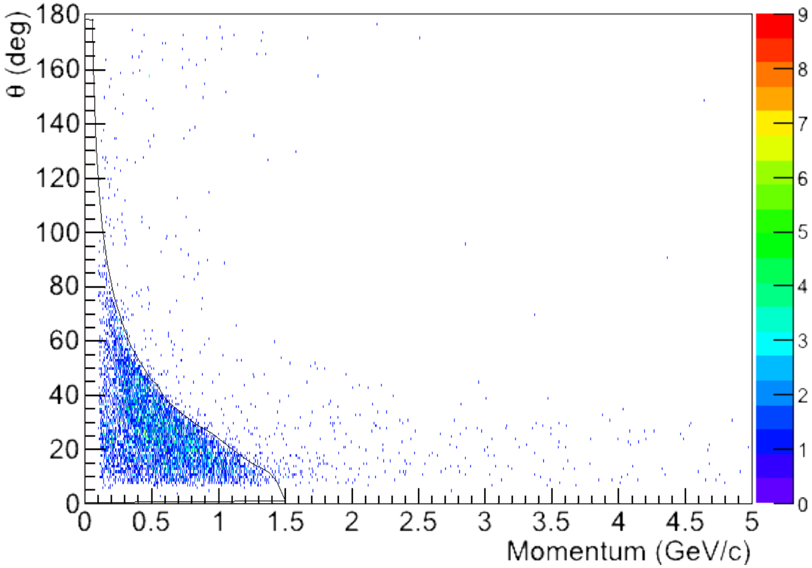

Kinematic selections (based on the Monte-Carlo truth) are required for the reconstruction of the electron decay of the J/ψ due to the more severe scattering and energy loss.

Particle Decays

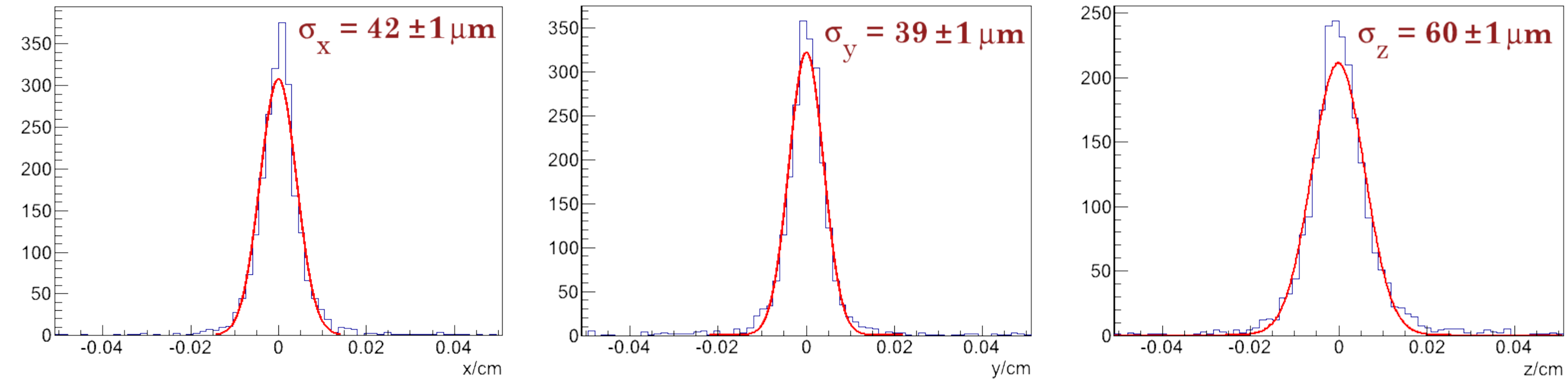

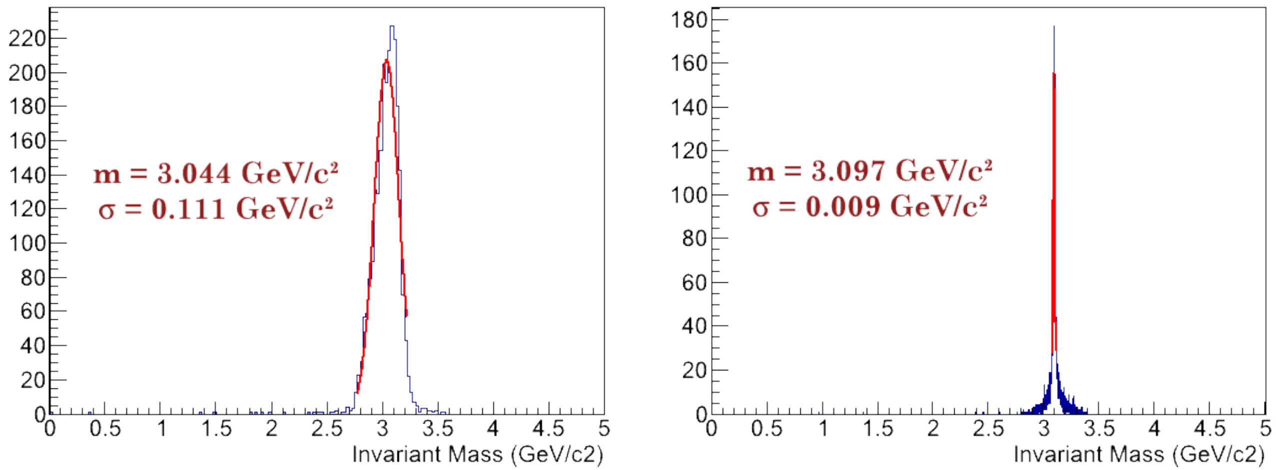

$J/\psi \rightarrow e^+e^-$ reconstructed vertices, invariant and missing mass.

The Bonn Tracking Station

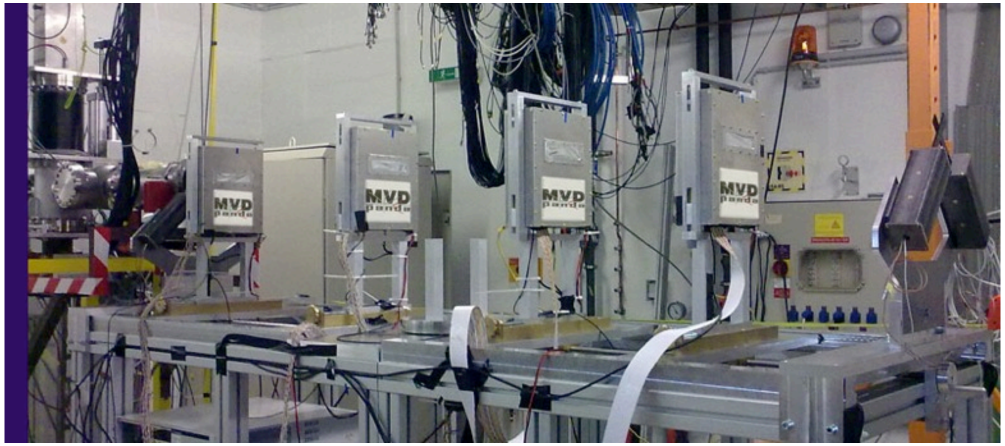

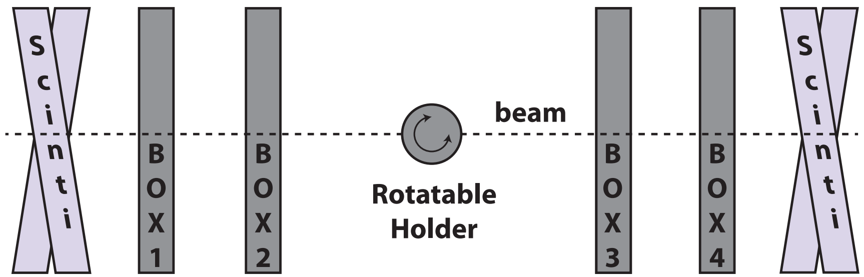

Four boxes are equipped with square silicon strip sensors.

Four scintillating slabs are used to trigger the data acquisition.

The boxes can be moved along a 2 m longitudinal span.

The position of each box can be adjusted in the 3 coordinates.

A fifth holder is foreseen which can be used to rotate one sensor or to place scattering volumes.

S. Bianco, M. Becker, K.-Th. Brinkmann, R. Kliemt, K. Koop, R. Schnell, T. Würschig, H.G. Zaunick, "Measurements with a Si-strip telescope", PoS (RD11) 025, http://pos.sissa.it/archive/conferences/143/025/RD11_025.pdf

Sensors and DAQ

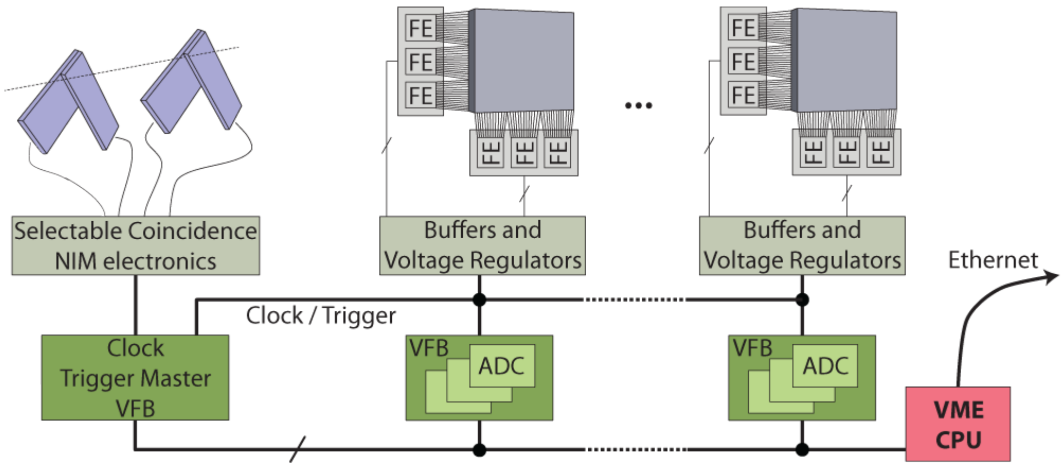

Sensors:

1.92 x 1.92 cm^2 active area
300 µm thick
50 µm strip pitch
90° stereo angle
Single/double sided

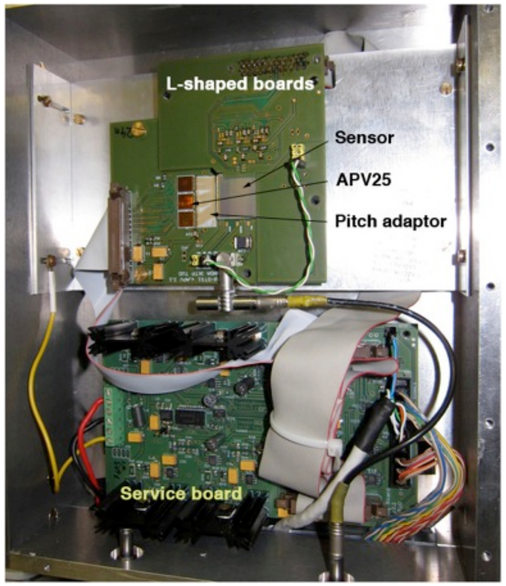

Read-out and DAQ

Sensors are read out with APV25 chips (128 ch each).

The analog output is sampled with ADC modules on FPGA boards on which online processing (baseline correction, clustering, …) can be performed.

Raw Data Conversion

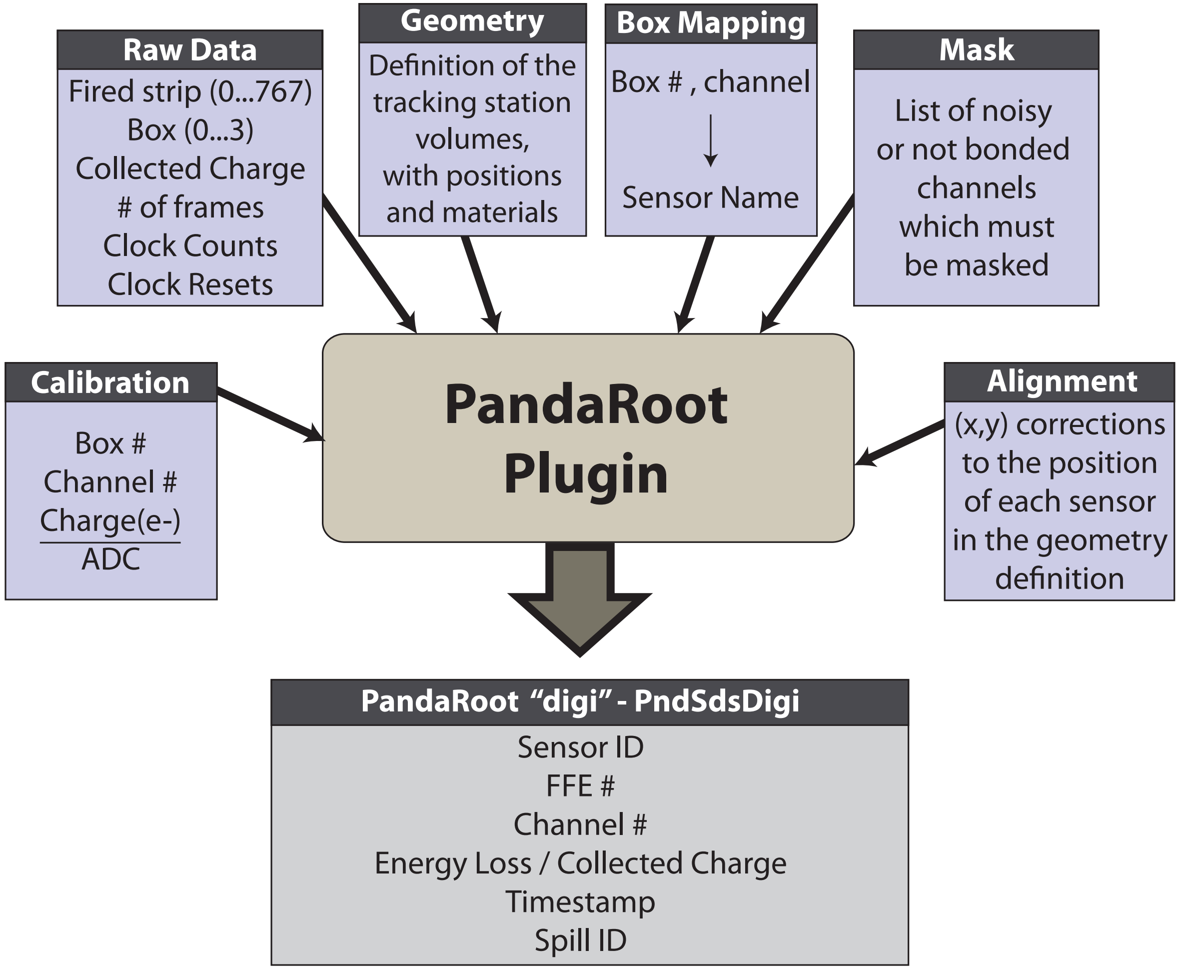

Goal: use the same tools to analyze measured and simulated data.

→ Raw data must be plugged into the framework before clustering.

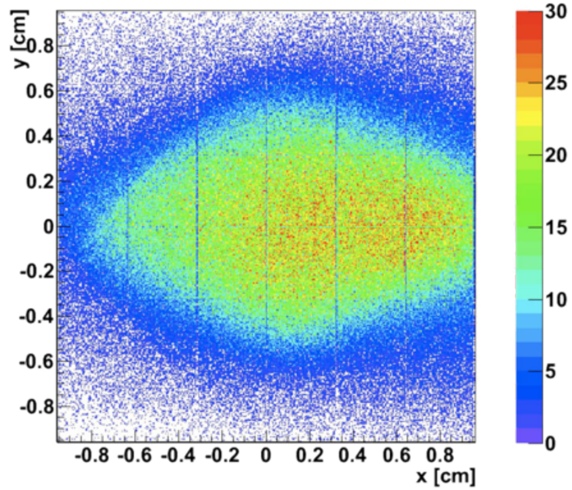

Energy Calibration and Iterative Alignment

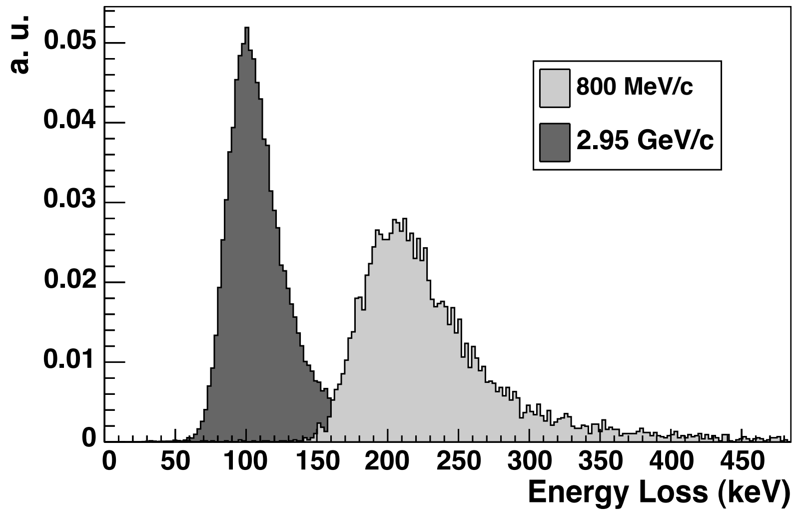

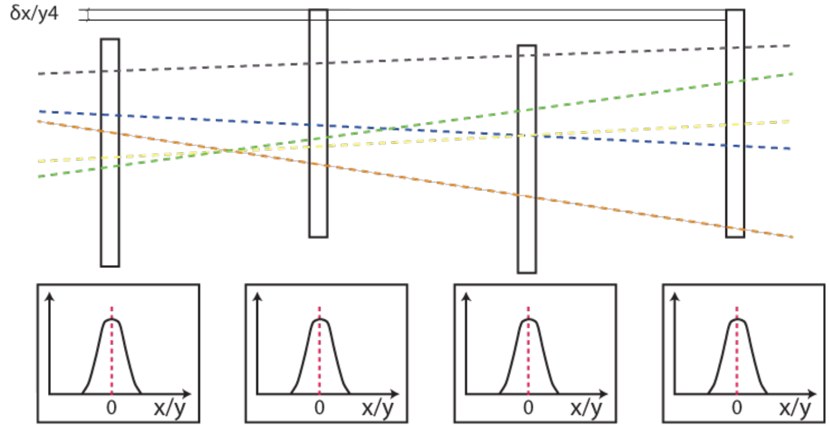

Energy calibration is performed in 2 steps:

- Injected charge
- MIP scaling

Off-line alignment is realized iteratively correcting the position of the sensors minimizing the mean of the exclusive residuals.

Rotations

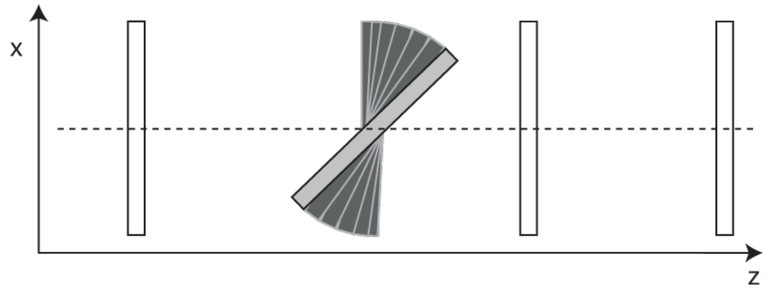

4 GeV electrons @ DESY (Hamburg)

One sensor rotated with respect to the plane orthogonal to the beam direction.

Bigger angles:

→ longer effective crossed length
→ expected growing energy loss per particle

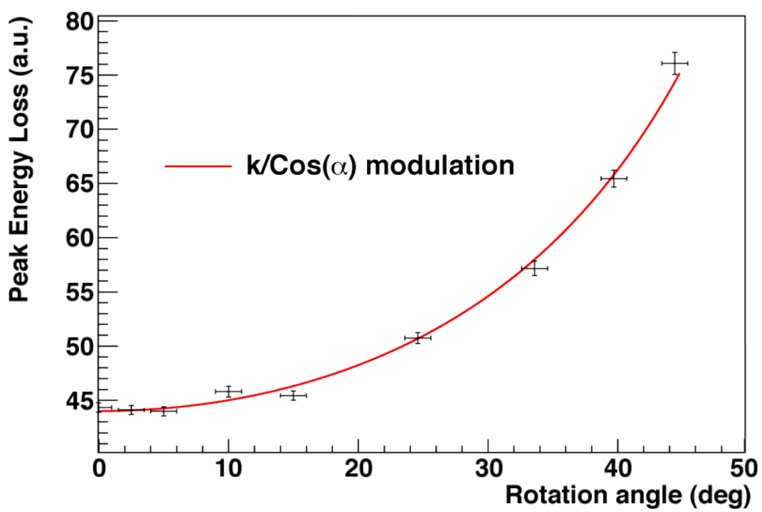

Results of the measurements:
MPV energy loss vs rotation angle

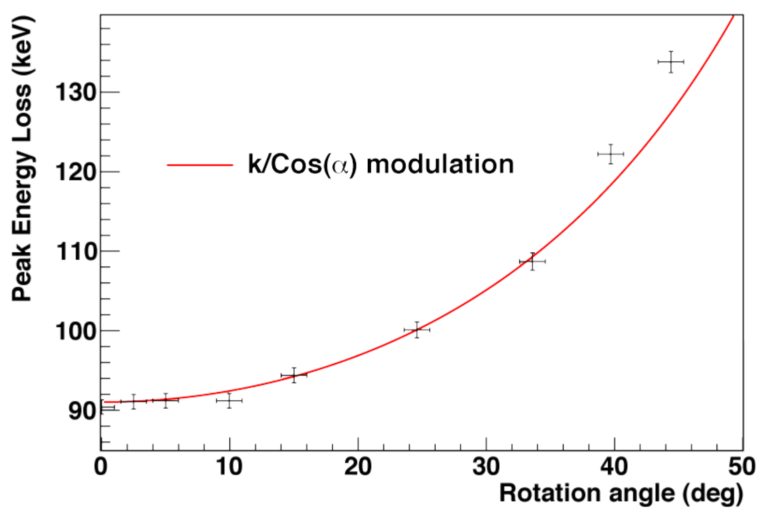

Simulation of the experimental setup
with the PandaRoot framework

Rotations

Rotations also influence the average cluster size: diverging from the orthogonal incidence the probability of firing more channels grows.

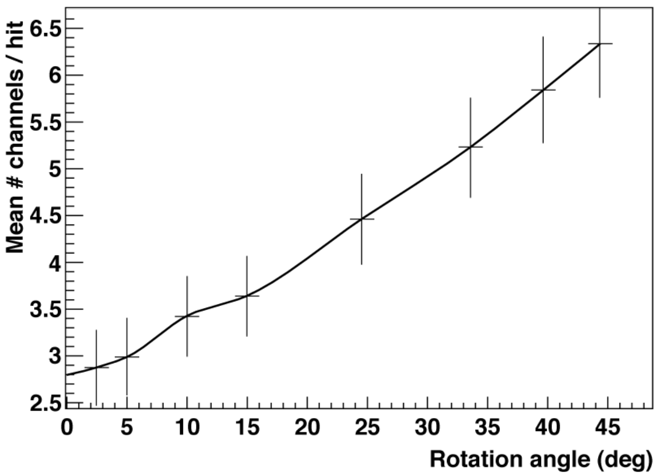

Results of the measurements: cluster size (# channels) Vs angle

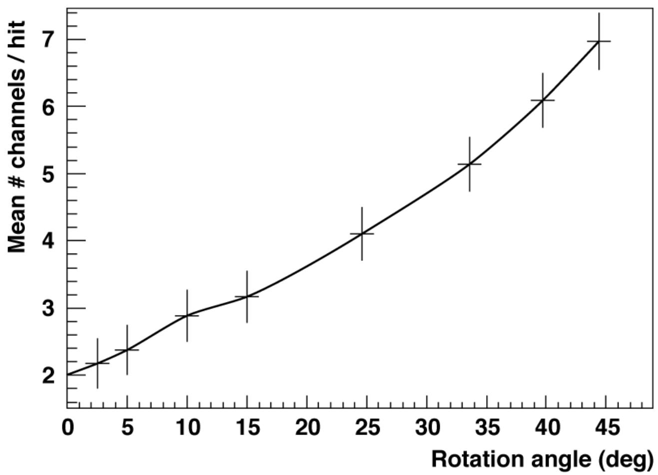

Simulations of the setup at the different experimental conditions

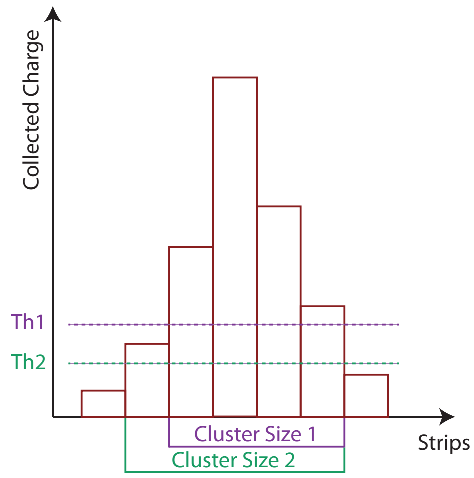

The enhancement at α ~ 9.5° corresponds to the angle necessary to span the width of a whole strip while crossing the sensor thickness:

α_C = arctan (pitch/thickness) = 9.46°.

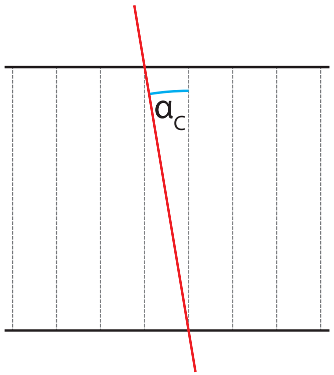

Scattering Measurements

Goals:

- Characterize the effect of light carbon foams on intermediate energy particle
- Validate the PandaRoot framework as a predictive tool for material effects estimates

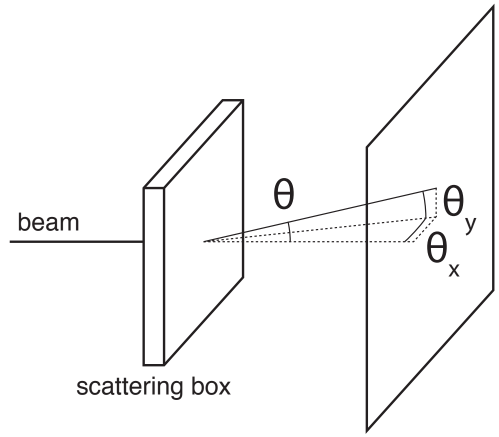

Setup: Two hit points are measured downstream and two upstream of the scattering volumes.

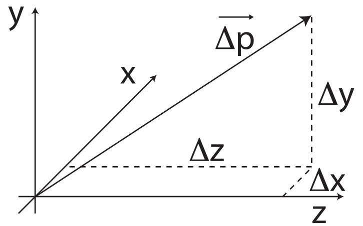

$$\theta_x = \arctan(\Delta x/\Delta z)$$
$$\theta_y = \arctan(\Delta y/\Delta z)$$

$$|\vec{p_i}| = |\vec{p_f}| = 1 \qquad \vec{\Delta p} = \frac{\vec{p_f} - \vec{p_i}}{|\vec{p_f} - \vec{p_i}|}$$

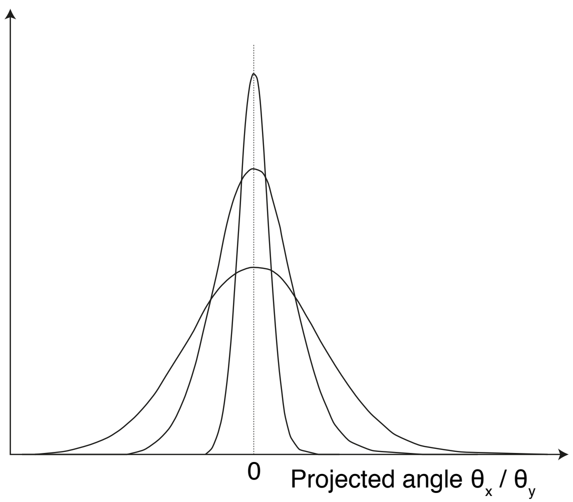

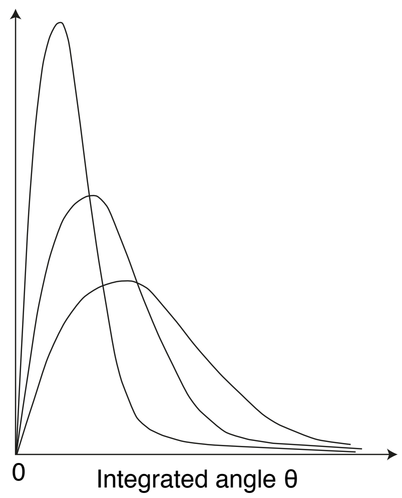

Scattering Measurements

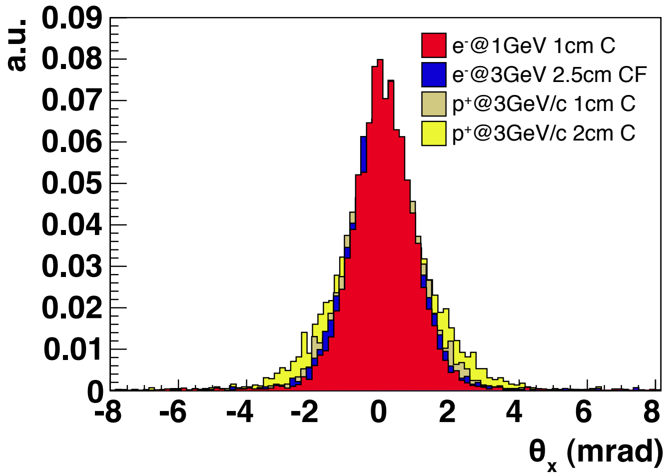

Element	Long. Position (cm)
Box1	11.0
Box2	80.7
Scatt. Vol.	115.0
Box3	139.0
Box4	227.3

Ptc	Mom. GeV/c	Volume	Thick. cm	X/X_0	σ_{meas} mrad	σ_{sim} mrad	Var. %
p^+	2.95	air	60	0.00197	0.532 ± 0.004	0.536 ± 0.002	0.75
p^+	2.95	1 cm C	1	0.042155	1.02 ± 0.01	1.01 ± 0.01	-0.98
p^+	2.95	2 cm C	2	0.079625	1.34 ± 0.01	1.33 ± 0.01	-0.74
e^-	1.	air	60	0.00197	1.24 ± 0.01	1.40 ± 0.01	12.9
e^-	2.	air	60	0.00197	0.622 ± 0.004	0.718 ± 0.003	15.4
e^-	3.	air	60	0.00197	0.423 ± 0.002	0.476 ± 0.002	12.5
e^-	4.	air	60	0.00197	0.325 ± 0.003	0.361 ± 0.002	11.1
e^-	5.4	air	60	0.00197	0.243 ± 0.003	0.284 ± 0.001	16.9
e^-	1	1 cm C	1	0.042155	2.48 ± 0.01	2.89 ± 0.01	16.5
e^-	5.4	1 cm C	1	0.042155	0.511 ± 0.004	0.599 ± 0.003	17.2
e^-	1	2 cm C	2	0.079625	3.15 ± 0.01	3.82 ± 0.02	21.3
e^-	5.4	2 cm C	2	0.079625	0.698 ± 0.002	0.807 ± 0.002	15.6
e^-	1	C-Foam	2.5	0.030445	2.18 ± 0.01	2.54 ± 0.01	16.5
e^-	3	C-Foam	2.5	0.030445	0.745 ± 0.003	0.887 ± 0.004	19.0
e^-	4	C-Foam	2.5	0.030445	0.588 ± 0.004	0.645 ± 0.003	9.7
e^-	1	Support Disk	0.4	0.0103	1.76 ± 0.01	1.87 ± 0.01	6.3
e^-	3	Support Disk	0.4	0.0103	0.600 ± 0.003	0.611 ± 0.002	1.8
e^-	4	Support Disk	0.4	0.0103	0.471 ± 0.004	0.483 ± 0.003	2.6
e^-	1	Carbon Foil	0.0650	0.00304	1.30 ± 0.01	1.56 ± 0.01	20.0
e^-	5	Carbon Foil	0.0650	0.00304	0.279 ± 0.002	0.334 ± 0.001	19.7

Excellent agreement between measurements and simulations for protons. The scattering of electrons is overestimated by the MC simulations, even though the scaling with X/X_0 is well respected.

Combined Pixels + Strips Beam Test

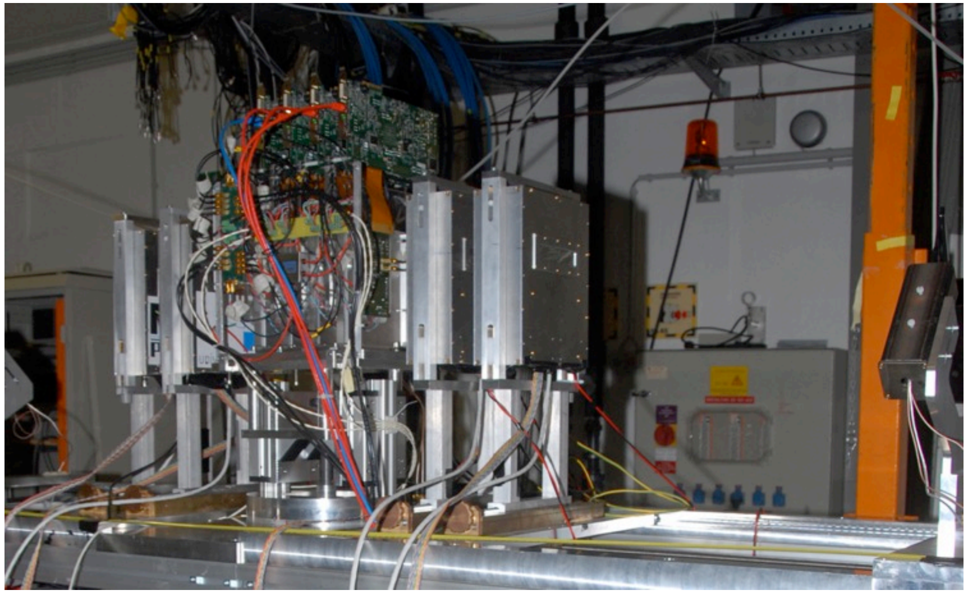

Si-strip + Si-pixel tracking stations with up to 4 sensors each.

The Si-strip sensors are triggered by the coincidence of scintillators.

Si-pixel modules are read-out with self-triggered front-end chips.

Beam test with 2.7 GeV/c protons at COSY (FZ Jülich).

A common 50 MHz clock and a reset (spill counter) signals are distributed to both systems for synchronization.

Different possible configurations:

- changes in the span between consecutive modules
- different number of sensors included

S. Bianco on behalf of the PANDA MVD group, "*Beam Tests and Performance Studies for the PANDA Micro-Vertex-Detector*", IEEE NSS Record N14(219), 2012, 1503-1508

The Pixel Telescope

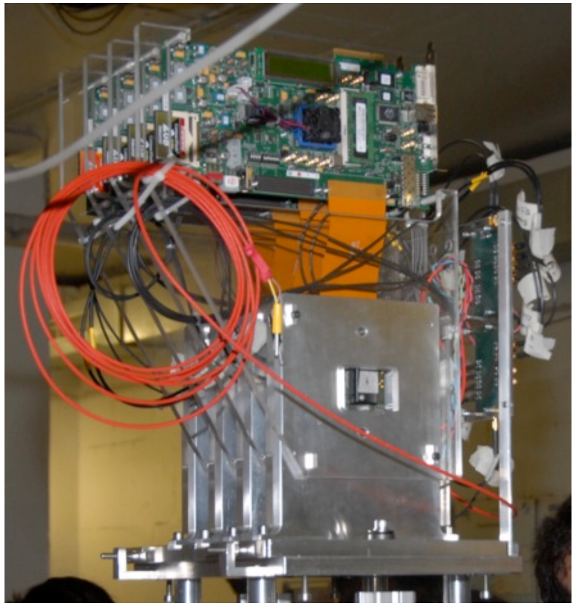
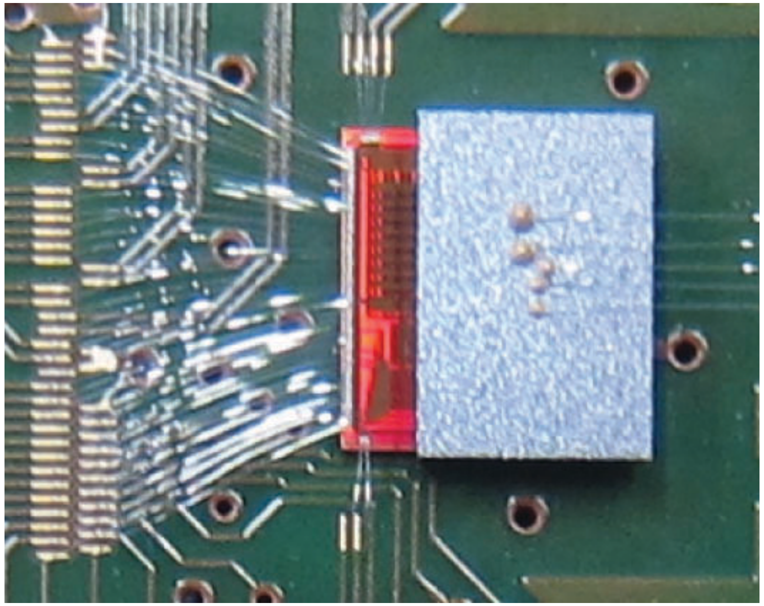
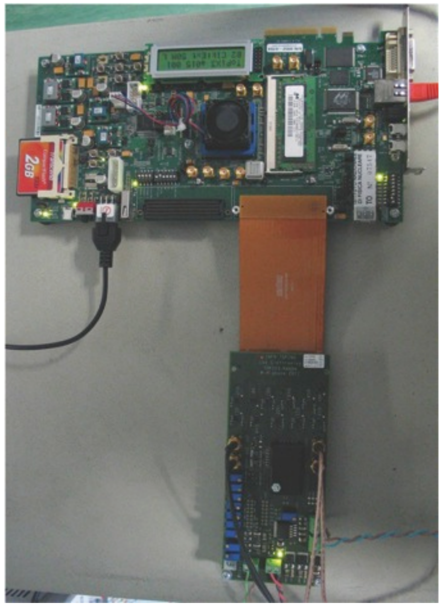

- 2.0 mm x 3.2 mm sensors with 100 μm x 100 μm pixel cells
- 100 μm epitaxial-Si sensors grown on a Cz-substrate (525 μm → 20 μm by thinning)
- ToPix3 prototype bump bonded to the sensors (300 μm thick)
- FPGA boards to read out the sensors

The Pixel Telescope

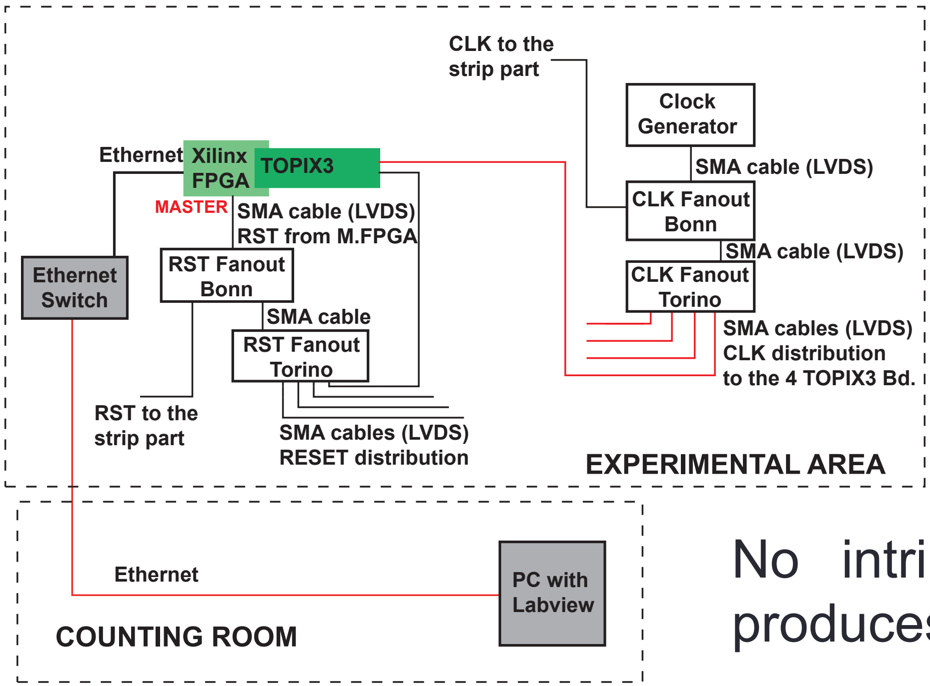

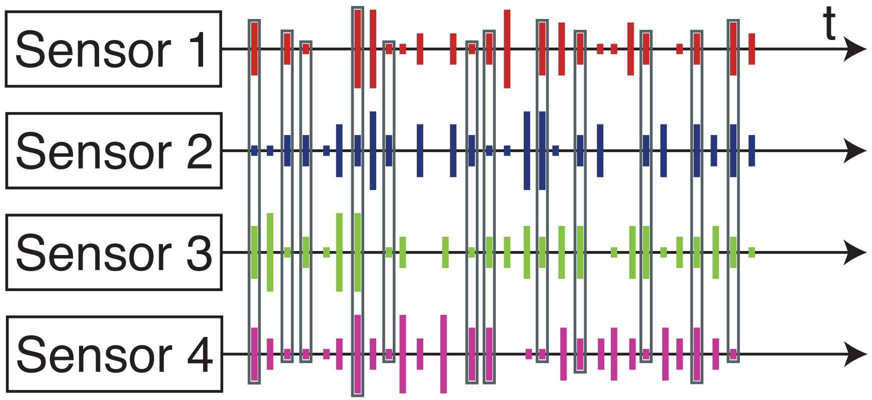

No intrinsic event structure: each sensor produces a flow of time ordered hits.

Event building can be performed looking at the timestamp (in terms of the common clock cycles) of the hits.

Sets of hits on the different sensors with compatible timestamp (±2 - 5 clock cycles @ 50 MHz = 40-100 ns) are assigned to one event.

Combined Event Building

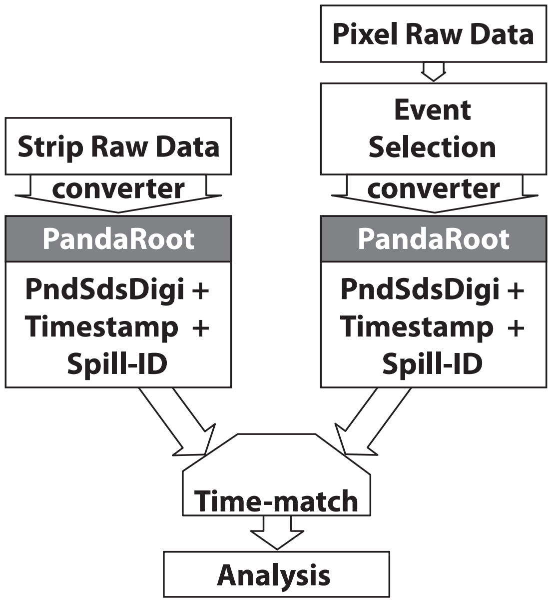

The global event building is performed **after** the cluster reconstruction on each system.

Two independent sets of events are available.

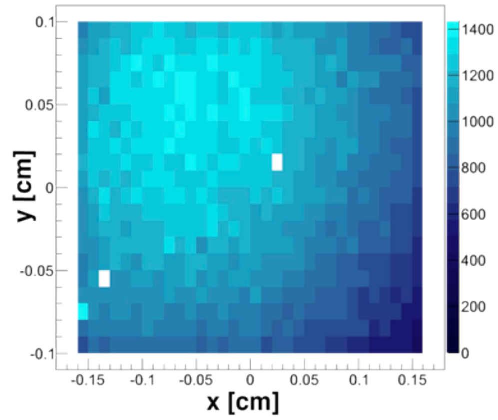

To distinguish real tracks from noisy hits or cosmic rays a matching procedure is used: only sub-events with the same spill ID and compatible timestamp are considered for the final analyses.

A precise synchronization of the two systems is required.

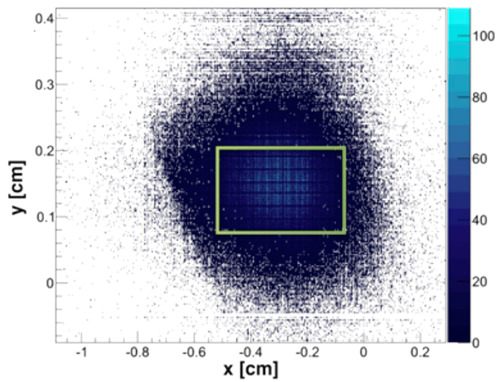

Timestamp Matching

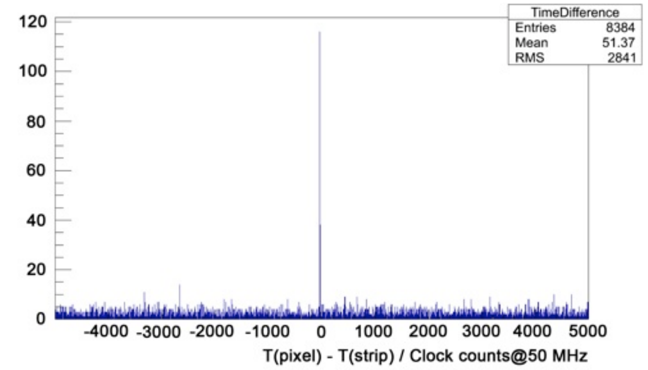

Δ-timestamp in all possible pixel-strip events combinations is plotted.

The peak corresponds to the correct global event assignments.

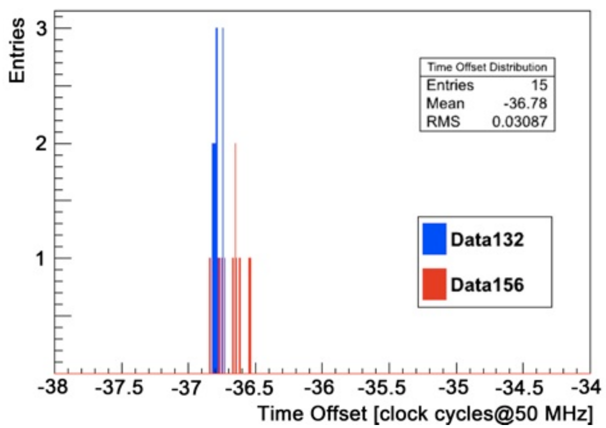

The position of the peak represents the offset between the acquired timestamp in the two systems → Constant within the beam test.

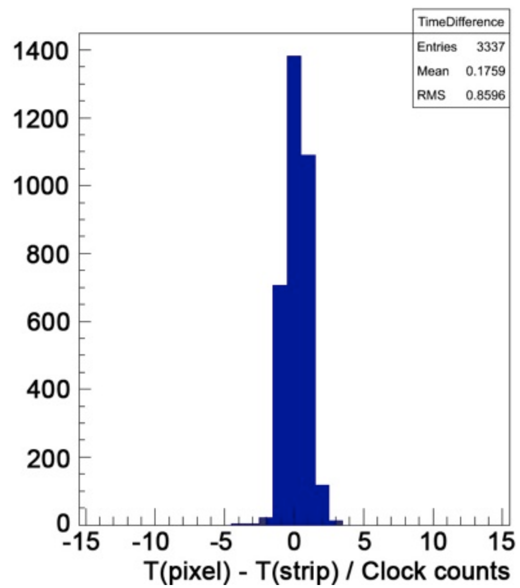

The timestamp offset correction is needed before applying the matching selection.

Results

Strip sensors

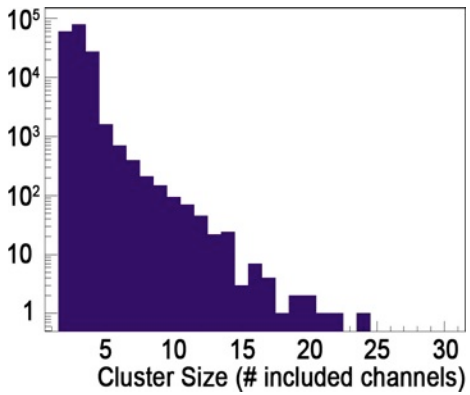

Pixel sensors

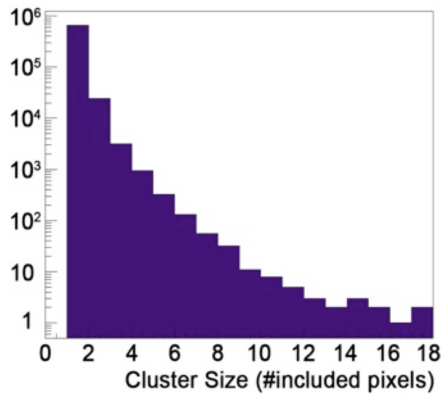

Tracks going through the whole TS are nearly orthogonal to the sensor surfaces.

→ small clusters

Strips: 2-3-4 ch./cluster

Pixels: mostly 1 ch./cluster

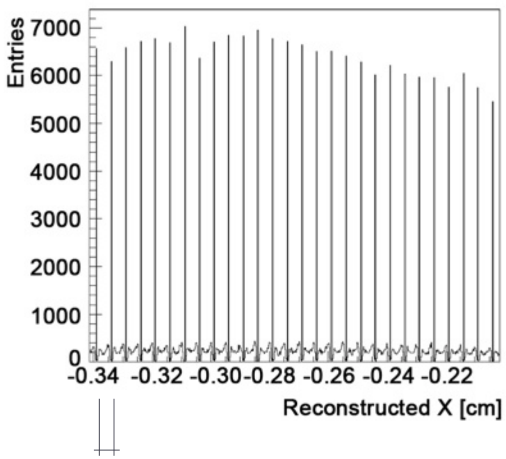

50 µm

The coordinate is reconstructed out of a single channel.

→ the measured position is at the center of the strip/pixel width

→ peaked structure of the reconstructed coordinate distributions

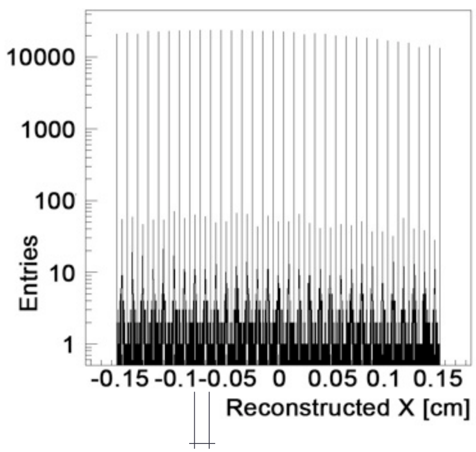

100 µm

Λ_C Reconstruction

$$\bar{p}\; p \rightarrow \Lambda_C^+\; \bar{\Lambda}_C^- \rightarrow p\; K^-\; \pi^+\;\; \bar{p}\; K^+\; \pi^-$$

$$p_{\bar{p}} = 15\ \mathrm{GeV/c}$$

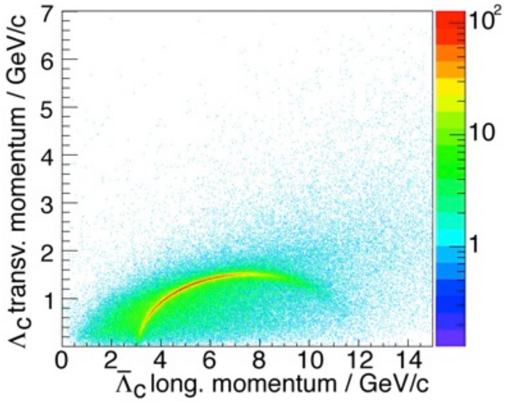

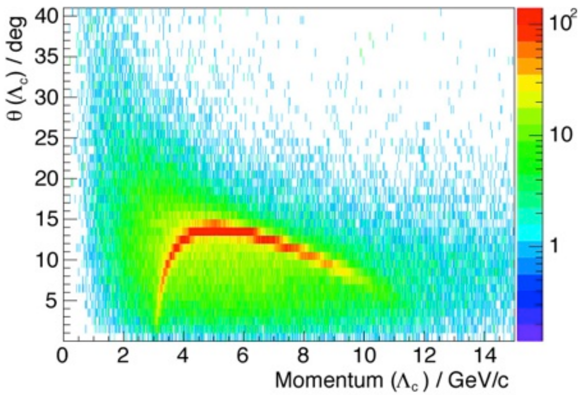

Maximum (15 GeV/c) beam momentum is chosen to maximize the opening angle between the Λ_C and the $\bar{\Lambda}_C$.

Reconstruction of the pure signal.

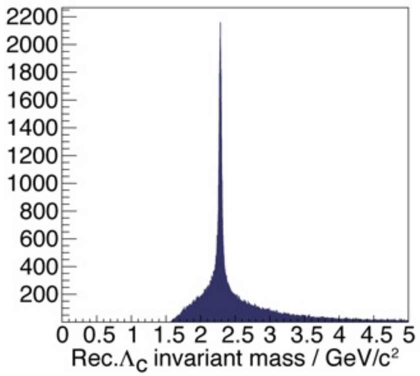

No selections

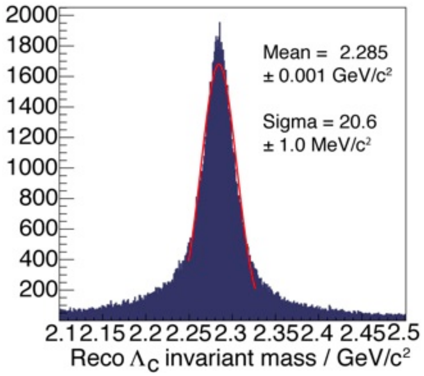

Kin. cuts

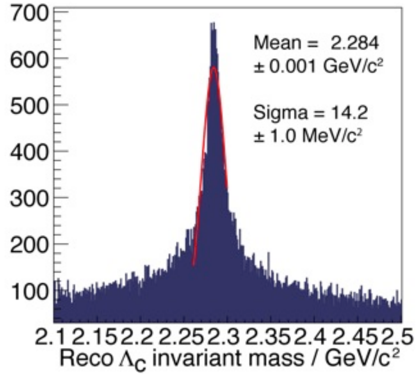

4 constraints fit

Coord.	Res.
x	59 μm
y	58 μm
z	179 μm

Λ_C Reconstruction

$\bar{p}\,p \rightarrow p\,K^-\,\pi^+\;\;\bar{p}\,K^+\,\pi^-$ $\qquad p_{\bar{p}} = 15\ \mathrm{GeV/c}$

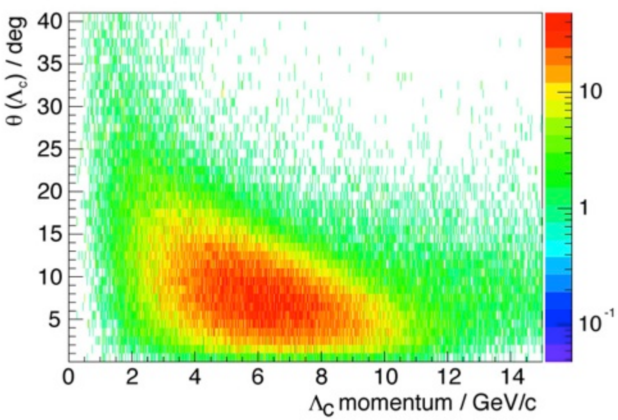

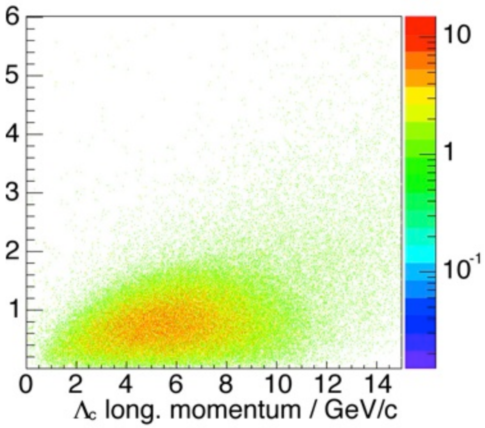

Non-resonant case: same final state, but not through the decays of the Λ_Cs.

The same kinematical cuts applied to the pure signal are used here.

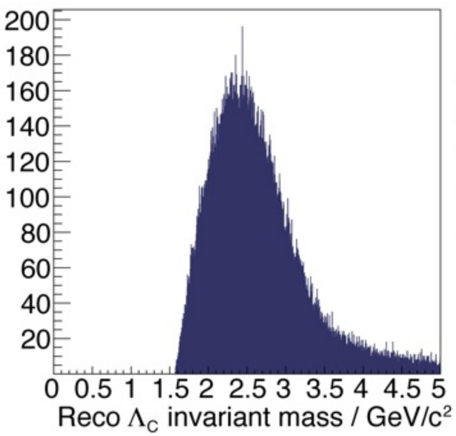

No selections

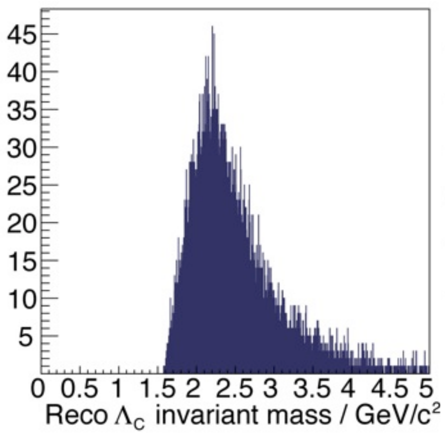

Kin. cuts

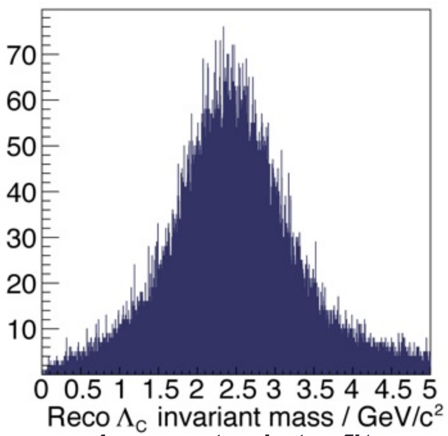

4 constraints fit

	Res	**Non-Res**
# Reco. Tracks	33.05%	8.0%
Peak	88.0%	11.4%

Suppression by the kinematic selections

Λ_C Reconstruction

From previous measurements the cross section for the non-resonant case can be extrapolated to be: $\sigma\left(\bar{p}p \rightarrow pk^-\pi^+\bar{p}k^+\pi^-\right)_{\sqrt{s}=5.474\ \mathrm{GeV}} = 20\ \mu b$

Theoretical calculations predict the $\Lambda_C\bar{\Lambda}_C$ production cross section:

$$\sigma\left(\bar{p}p \rightarrow \Lambda_C\bar{\Lambda}_C\right)_{\sqrt{s}=5.474\mathrm{GeV}} = 200\ \mathrm{nb}$$

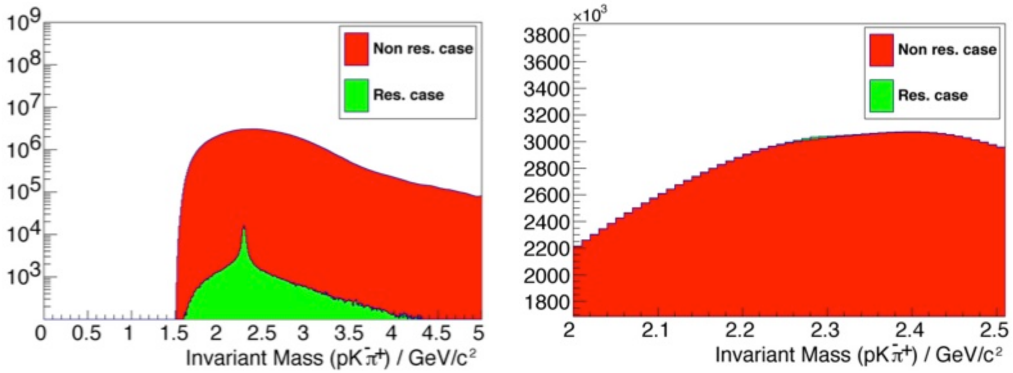

Without selections

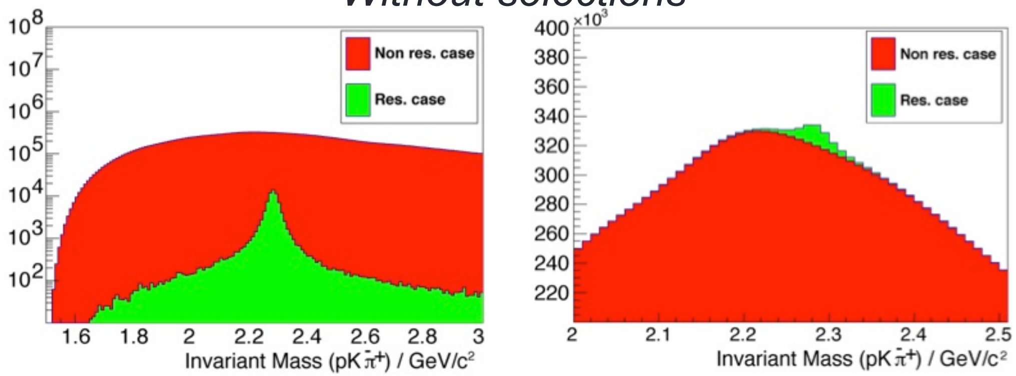

With kinematic cuts

Since the BR for $\Lambda_C \rightarrow pk^-\pi^+$ is 5% a scaling factor of 2000 was used to compare resonant and non-resonant statistics.

The kinematical cuts allow to distinguish the Λ_C from the non-resonant background.

Conclusions

- The geometry of the MVD has been imported in the simulation framework allowing for a detailed characterization.
- The vertex reconstruction performance of the MVD was characterized with systematic scans and with a particle decay benchmark.
- A tracking station (TS) equipped with silicon strip sensors has been tested at several beam facilities studying the effects of variations in the setup and realizing scattering measurements.
- A combined beam test with the Torino pixel sensor telescope allowed to test the synchronous operation of the TS with a trigger-less system.
- An event building procedure was implemented to allow global event reconstruction.
- The MVD proved to play a key role in the reconstruction of particle momenta and vertices enabling the study of short-lived particles such as the Λ_C.

Thanks for your attention